The Crystal Structure of Ferrioxamine E

Dick van der Helm* and M. Poling

Contribution from the Department of Chemistry, University of Oklahoma, Norman, Oklahoma, 73069. *Received March 27, 1975*

Abstract: The crystal structure of ferrioxamine E, $C_{27}H_{45}N_6O_9Fe \cdot 1.5H_2O$, has been determined with single-crystal x-ray diffraction. The crystals are triclinic, space group $P\bar{1}$, two molecules per unit cell with dimensions a = 19.77 (1) Å, b = 10.512 (2) Å, c = 8.029 (2) Å, α = 106.84 (2)°, β = 93.91 (2)°, and γ = 97.74 (3)°. The intensity data (3963) were collected on an automatic diffractometer. The structure, determined by the heavy-atom method, was refined by least-squares methods. The final R was 0.076 for all data. The Fe^{3+} ion is coordinated in a cis configuration to three hydroxamate groups. The molecule is quite flat with a total thickness of 3.6 Å. The peptide carbonyl bonds are approximately perpendicular to the plane of the molecule and all point in the same direction.

Most aerobic microorganisms contain compounds which solubilize and transport iron(III). These low molecular weight compounds are called siderochromes. The subject has recently been reviewed by Neilands[1] and Emery.[2] The stability constants of deferrisiderochromes, the ligands, with iron(III) are of the order of 10^{30}, while they have little or no affinity for iron(II). The compounds are separated into families in which the iron binding atoms may be furnished by hydroxamic acid groups, carboxylic acid and hydroxyl group, or catechol residues. All siderochromes contain peptide linkages which are not coordinated to the iron(III) atom. The families are ferrioxamines, ferrichromes, enterobactins, fusarinines, rhodotoluric acids, and aerobactins. Many of the compounds show either growth-factor or antibiotic activity.

The first isolation and characterization of a siderchrome was performed by Neilands for ferrichrome.[3] The compound showed potent growth-factor activity. An important discovery was also the fact that deferrisiderochromes are produced in high yield in the medium when the organisms are grown under conditions of low iron stress.[4,5] This observation together with the high stability constants of siderochromes and other evidence led Neilands to suggest that these compounds act as cellular transport agents for iron in aerobic microorganisms.[6] At the present time there is also substantial evidence for a process of "active" transport of siderochromes across the membrane into the cell.[1,7]

The ferrioxamines are metabolic products of actinomycetes and were originally isolated and characterized as ferrioxamines A, B, C, D_1, D_2, E, F, and G by a group of workers in Switzerland.[8,9] All ferrioxamines are trihydroxamates and the deferrioxamines are either cyclic (D_2 and E) or linear. The chemical structures of the ferrioxamines are known. The structures were established by degradation methods and chemical syntheses by Keller-Schierlein, Prelog and co-workers.[9-15]

In exchange experiments Emery showed,[16] in ferrichrome and also in ferrioxamine, that a drastic conformational change must occur upon chelation of iron. The conformational change in the ligand has also been studied by NMR in the ferrichrome series.[17] The conformational change between complexed and free ligand may furnish a selective device at the cell surface for excretion of the deferrisiderochrome into the medium and the transport of the siderochrome itself into the cell. It is therefore our purpose to study the structure of the siderochromes and deferrisiderochromes by single-crystal x-ray diffraction, and to compare the conformations. The structure of ferrioxamine E, $FeC_{27}H_{45}N_6O_9$ (Figure 1), was determined and is reported in this paper.

The structure of ferrichrome A has been reported previously by Zalkin, Forrester, and Templeton.[18] This molecule contains a hexapeptide while the iron is bound by three hydroxamate groups. The structure of one other iron(III) hydroxamate, in this case a synthetic compound, has been determined.[19]

Experimental Section

Crystallization and Crystal Data of Ferrioxamine E. A microcrystalline sample of the compound was received from Dr. W. Keller-Schierlein of the Eidg. Technische Hochschule in Zurich, Switzerland. Slow evaporation from aqueous solutions yielded the best crystals, but in general the crystals showed large mosaicity. A data crystal was obtained in the shape of a plate with dimensions of 0.25 × 0.24 × 0.024 mm. The mosaic spread of this crystal was 1.3° measured at the peak base using an ω-scan. Initial oscillation and Weissenburg exposures showed the crystal to be triclinic. The crystal data are: $C_{27}H_{45}N_6O_9Fe \cdot 1.5H_2O$; M = 680.6; triclinic; a = 19.77 (1), b = 10.512 (2), c = 8.029 (2) Å; α = 106.84 (2)°, β = 93.91 (2)°, γ = 97.74 (3)°; V = 1572 Å^3; Z = 2; ρ_{calcd} = 1.44, ρ_{obsd} = 1.38 g cm^{-3}; $F(000)$ = 724; space group $P\bar{1}$ as confirmed by structure determination; nickel filtered Cu Kα radiation: λ(Cu Kα_1) 1.54051 Å for 2θ-data and λ(Cu Kα) 1.5418 Å for intensity data; μ(Cu K$\bar{\alpha}$) = 44.1 cm^{-1}.

The cell parameters were determined by a least-squares fit to the + and − 2θ values of 32 reflections distributed throughout all of reciprocal space. The observed density was measured by the flotation method in a mixture of hexane and carbon tetrachloride. The discrepancy between the calculated and observed density corresponds to 1.5 molecule of H_2O per molecule of ferrioxamine, and the difference therefore is probably caused by the loss of water of hydration from the sample in the density measurement.

The intensities of all 3963 unique reflections with $\theta \leq 55°$ were measured on a Nonius CAD-4 automatic diffractometer using a θ-2θ scan technique. The scan widths ($\Delta\theta$) were adjusted to the dispersion and calculated with the formula $\theta° = (1.5 + 0.15 \tan \theta)°$, for each reflection. A horizontal receiving aperture with a variable width (width (mm) = 5 + 0.5 tan θ), and height of 6 mm, was located 173 mm from the crystal. A reflection was scanned for a maximum time of 180 sec, with two-thirds of the time spent on scanning the peak (P) and one-sixth of the time spent on each the high- and low-θ backgrounds (LH and RH). The unscaled intensities (I) were calculated as $I = P - 2(RH + LH)$. The scan time was less than 180 sec for those intensities where a value of 50000 for I could be attained with a faster scan speed than the normal one of 1.5°/min. A standard reflection was monitored after every 20 measurements.

The intensity of the monitor reflection decreased 11% during the 11-day period needed for the data collection. The change appeared to be continuous over fairly long time periods. The monitor reflections were used to bring the intensities on a common scale. The orientation of three reflections was automatically checked after every 50 measurements. In the case that the 2θ, ω, ϕ, or χ angles of these three reflections were changed by more than 0.1°, automatically a new orientation matrix was obtained using a list of 11 reflections. There were 815 reflections which could not be distinguished from the background on the basis that the intensity (I) was less than

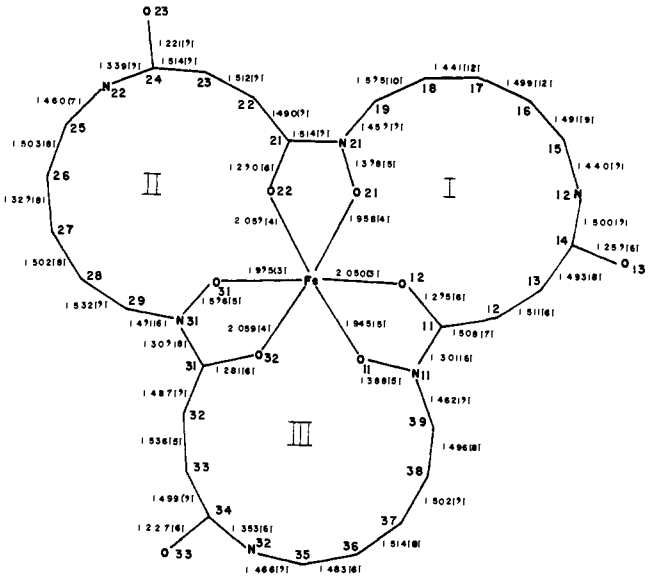

Figure 1. The numbering used in ferrioxamine E and the bond distances. Standard deviation for the last digit is in parentheses. The Fe-O distances (Å) corrected for thermal motion (riding) are: Fe-O(11), 1.949; Fe-O(12), 2.053; Fe-O(21), 1.946; Fe-O(22), 2.059; Fe-O(31), 1.978; Fe-O(32), 2.061.

$2(T)^{1/2}$ (T = [P + 2(RH + LH)]). These reflections were assigned intensities equal to $T^{1/2}$ for the purpose of least-squares refinement. Lorentz, polarization, and absorption corrections were applied to the data. A Gaussian method[20] was employed to make the absorption correction, by using 216 sampling points. The absorption coefficients varied between 0.47 and 0.90. Each structure amplitude was assigned a weight given by $w_F = 1/\sigma_F^2$ where the standard deviation σ_F of the amplitude is given by

$$\sigma_F = \tfrac{1}{2}\left[\frac{\sigma^2 + (0.06I\nu)^2}{(\mathrm{Lp})(I\nu)}\right]^{1/2}$$

$\sigma = (T^{1/2})\nu$. ν is scan speed and Lp is the Lorentz-polarization factor.

Structure Determination and Refinement. A sharpened Patterson synthesis was calculated in which the Fe-Fe vector was easily identified. The position of the Fe atom was used in a structure factor calculation and a subsequent difference Fourier synthesis revealed the positions of the six oxygen atoms coordinated to the Fe atom. Successive cycles yielded the positions of all other nonhydrogen atoms of ferrioxamine E and the position of a water molecule. At a later stage of refinement an additional disordered water molecule of hydration was located close to a center of symmetry. All nonhydrogen atoms were refined anistropically with block-diagonal (9 × 9) least-squares[21] methods. Near the end of the refinement the contributions of the hydrogen atoms were included in the structure factor calculations. Their locations were determined from geometrical considerations and their positions were confirmed in a difference Fourier with the exception of those bonded to C(16), C(17), and C(18). The hydrogen atom positions were not refined. The observed structure factors were corrected,[22] in each least-squares cycle, for the anomolous scattering of Cu radiation by the Fe atom.[23] During the refinement it became obvious that atoms C(16), C(17), and C(18) had large thermal motion or were disordered. An attempt to refine with two different sets of locations failed due to insufficient resolution of the available data. The root mean square amplitude of vibration along the major axis of the thermal ellipsoids for C(16), C(17), and C(18) as calculated from the final parameters are 0.175, 0.163, and 0.239 Å^2, respectively, while for the other atoms in ferrioxamine this value is always less than 0.100 Å^2 and for the large majority is less than 0.065 Å^2.

The scattering factors used were from the International Tables for X-Ray Crystallography.[23] The Fe^{3+}-ion scattering factor was used for the Fe atom, and in the hydroxamate groups the O^- form factors were used for the oxime oxygen atoms, while for all other atoms the scattering factors of the neutral atom were used. The

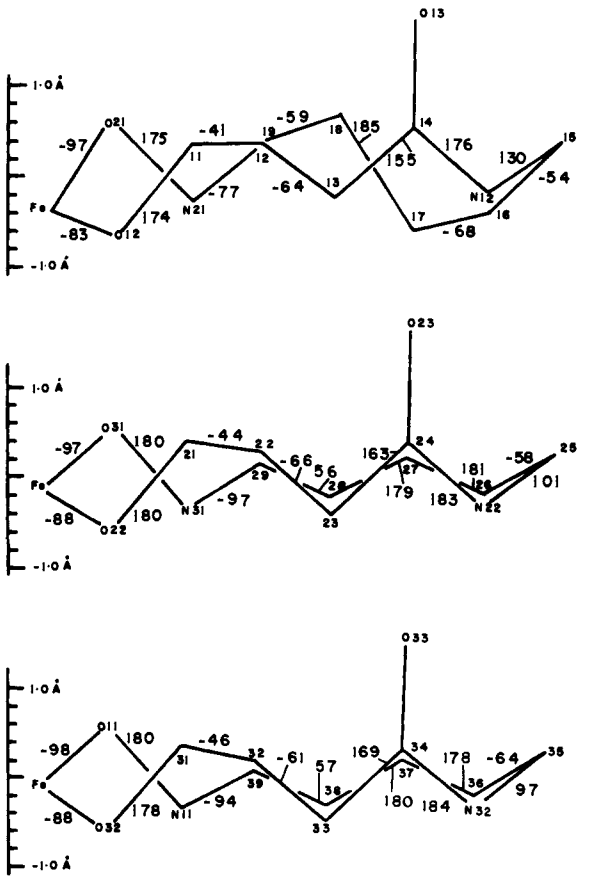

Figure 3. The torsion angles in macrocycles I, II, and III. The vertical elevations describe the distances from the least-squares planes through the rings.

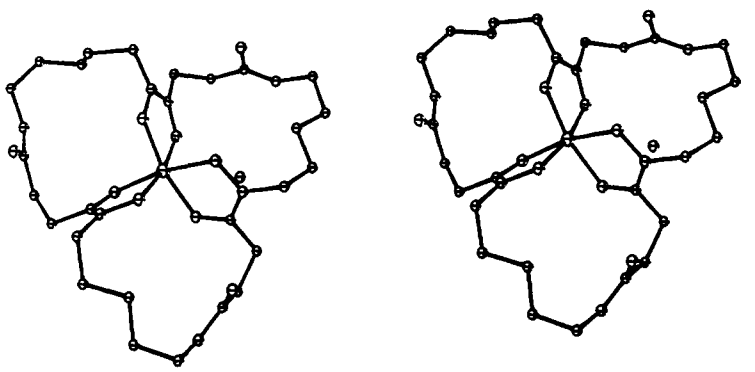

Figure 2. A three-dimensional view of ferrioxamine E, using the ORTEP program.[27] Macrocycle I is on top left, II top right, and III below. W(1) is also drawn.

Table I. Final Fractional Coordinates and Anisotropic Thermal Parameters for Nonhydrogen Atoms[a]

	x	y	z	U_{11}	U_{22}	U_{33}	U_{12}	U_{13}	U_{23}
Fe	2292.1 (4)	1581.5 (7)	977.7 (9)	30.1 (4)	26.3 (4)	31.8 (4)	7.7 (3)	4.8 (3)	8.4 (3)
C(11)	1665 (2)	3166 (5)	−726 (6)	25 (3)	26 (3)	34 (3)	2 (2)	1 (2)	8 (2)
C(12)	1403 (2)	3740 (5)	−2117 (6)	34 (3)	36 (3)	38 (3)	10 (2)	−1 (2)	13 (2)
C(13)	1825 (3)	3541 (5)	−3645 (6)	42 (3)	37 (3)	35 (3)	8 (3)	−3 (2)	13 (2)
C(14)	2547 (3)	4267 (5)	−3168 (6)	45 (3)	27 (3)	40 (3)	6 (2)	4 (2)	14 (2)
C(15)	3706 (3)	4356 (6)	−4026 (8)	46 (4)	59 (4)	73 (4)	9 (3)	15 (3)	24 (3)
C(16)	4179 (3)	3366 (8)	−4017 (11)	50 (4)	107 (6)	148 (7)	9 (4)	19 (4)	95 (6)
C(17)	4128 (4)	2579 (8)	−2730 (12)	73 (5)	96 (6)	158 (8)	21 (5)	37 (5)	62 (6)
C(18)	4325 (4)	3360 (7)	−923 (9)	120 (6)	70 (5)	74 (5)	−56 (5)	65 (5)	−18 (4)
C(19)	4346 (3)	2583 (6)	485 (8)	25 (3)	52 (4)	80 (4)	−1 (3)	10 (3)	0 (3)
N(11)	1689 (2)	3815 (4)	931 (5)	36 (2)	28 (2)	31 (2)	11 (2)	4 (2)	9 (2)
N(12)	2995 (2)	3769 (5)	−4177 (5)	42 (3)	48 (3)	47 (3)	4 (2)	11 (2)	1 (2)
O(11)	1927 (2)	3202 (3)	2123 (4)	43 (2)	35 (2)	25 (2)	15 (2)	4 (2)	5 (2)
O(12)	1877 (2)	2035 (3)	−1149 (4)	42 (2)	29 (2)	32 (2)	15 (2)	5 (2)	10 (2)
O(13)	2692 (2)	5307 (4)	−1915 (5)	48 (2)	37 (2)	67 (3)	−2 (2)	8 (2)	−15 (2)
C(21)	3427 (2)	552 (5)	−471 (6)	32 (3)	33 (3)	33 (3)	10 (2)	10 (2)	12 (2)
C(22)	3885 (3)	−340 (5)	−1456 (7)	39 (3)	37 (3)	50 (3)	10 (3)	11 (3)	13 (3)
C(23)	3775 (3)	−1750 (5)	−1298 (6)	36 (3)	50 (4)	40 (3)	14 (3)	4 (2)	5 (3)
C(24)	3965 (3)	−1769 (5)	553 (7)	34 (3)	47 (3)	47 (3)	15 (3)	3 (3)	6 (3)
C(25)	3803 (3)	−3105 (6)	2603 (7)	47 (4)	57 (4)	57 (4)	19 (3)	6 (3)	25 (3)
C(26)	3173 (3)	−2942 (6)	3538 (7)	54 (4)	47 (4)	57 (4)	25 (3)	4 (3)	21 (3)
C(27)	2949 (3)	−1568 (5)	3811 (6)	47 (3)	42 (3)	39 (3)	16 (3)	7 (3)	14 (3)
C(28)	2322 (3)	−1451 (5)	4768 (6)	53 (4)	39 (3)	36 (3)	11 (3)	4 (3)	17 (3)
C(29)	2078 (2)	−86 (5)	5096 (6)	44 (3)	41 (3)	29 (3)	8 (3)	8 (2)	12 (2)
N(21)	3672 (2)	1808 (4)	429 (5)	28 (2)	35 (3)	46 (3)	7 (2)	4 (2)	7 (2)
N(22)	3712 (2)	−2908 (4)	880 (5)	51 (3)	36 (3)	44 (3)	11 (2)	3 (2)	12 (2)
O(21)	3208 (2)	2590 (3)	1221 (4)	34 (2)	29 (2)	51 (2)	6 (2)	9 (2)	4 (2)
O(22)	2791 (2)	132 (3)	−509 (4)	31 (2)	28 (2)	41 (2)	7 (2)	8 (2)	12 (2)
O(23)	4347 (2)	−842 (4)	1629 (5)	57 (3)	56 (3)	62 (3)	−8 (2)	−17 (2)	8 (2)
C(31)	1422 (2)	−157 (5)	2268 (6)	31 (3)	26 (3)	36 (3)	9 (2)	1 (2)	5 (2)
C(32)	831 (3)	−1102 (5)	2497 (6)	43 (3)	32 (3)	38 (3)	6 (2)	3 (2)	13 (2)
C(33)	134 (3)	−723 (5)	2033 (6)	40 (3)	38 (3)	41 (3)	−4 (3)	3 (3)	10 (3)
C(34)	50 (2)	645 (5)	3163 (6)	32 (3)	39 (3)	34 (3)	−5 (2)	10 (2)	15 (2)
C(35)	−630 (3)	2492 (6)	3493 (7)	33 (3)	64 (4)	54 (4)	15 (3)	13 (3)	17 (3)
C(36)	−372 (3)	3506 (5)	2633 (7)	45 (3)	48 (4)	47 (3)	21 (3)	13 (3)	13 (3)
C(37)	401 (3)	3751 (5)	2652 (6)	40 (3)	42 (3)	43 (3)	13 (3)	6 (3)	7 (3)
C(38)	644 (3)	4751 (5)	1725 (6)	47 (3)	37 (3)	45 (3)	19 (3)	12 (3)	9 (3)
C(39)	1406 (3)	5037 (5)	1718 (7)	42 (3)	24 (3)	52 (3)	10 (2)	11 (3)	8 (2)
N(31)	1948 (2)	276 (4)	3478 (5)	34 (2)	30 (2)	30 (2)	8 (2)	10 (2)	12 (2)
N(32)	−494 (2)	1135 (4)	2617 (5)	29 (2)	44 (3)	44 (3)	2 (2)	0 (2)	9 (2)
O(31)	2484 (2)	1122 (3)	3162 (4)	30 (2)	33 (2)	34 (2)	6 (2)	2 (2)	10 (2)
O(32)	1429 (2)	215 (3)	883 (4)	32 (2)	33 (2)	35 (2)	5 (2)	−2 (2)	14 (2)
O(33)	446 (2)	1260 (3)	4482 (4)	43 (2)	43 (2)	35 (2)	0 (2)	−6 (2)	3 (2)
W(1)	1958 (2)	−2559 (4)	−551 (6)	48 (3)	58 (3)	109 (4)	11 (2)	13 (2)	19 (3)
W(2)[b]	4857 (12)	−506 (22)	5224 (26)	178 (19)	241 (30)	119 (13)	−77 (15)	−28 (12)	−25 (16)

[a] The x, y, and z (all x10⁴) are fractional coordinates. The anistropic parameters (Å², all x10³) are used in the expression: $\exp(-[2\pi^2(U_{11}h^2a^{*2} + U_{22}k^2b^{*2} + U_{33}l^2c^{*2} + 2U_{12}hka^*b^* + 2U_{13}hla^*c^* + 2U_{23}klb^*c^*)])$. Standard deviation for the last digit is in parentheses. [b] Disordered water molecule with 0.50 occupancy.

choice to put the anion charge on the oxime oxygen atoms was confirmed by the final results in that all oxygen atoms in the three hydroxamate groups showed approximately the same thermal motion, while also the bond distances agreed with this model (vide infra).

The final R value $R = \sum||kF_o| - |F_c||/\sum|kF_o|$ is 0.076 for all 3963 data and 0.055 for the 3148 data with intensities above background. The data with intensities not discernible from background were only included in the least-squares calculations when $|F_c| > 2F_o$.[24] The least-squares calculations minimized the quantity $\sum w_F(kF_o - F_c)^2$. The mean values of $w_F\Delta F^2$ calculated for various ranges of $|F_o|$ were quite constant validating the weighting scheme used. The final difference Fourier showed peaks between −0.5 and +0.4 eÅ^{-3} around C(16), C(17), and C(18), between −0.3 and + 0.4 eÅ^{-3} around the Fe atom and between −0.4 and +0.2 eÅ^{-3} around the disordered water molecule. All other peaks were less than 0.3 eÅ^{-3}.

The final parameters for the nonhydrogen atoms are shown in Table I. The observed and calculated structure factors are available.[25]

Results and Discussion

A stereoview of ferrioxamine E is shown in Figure 2. The bond distances and atom numbering are given in Figure 1. The bond angles are listed in Table II. Keller-Schierlein and Prelog originally speculated about the stereochemistry of iron-chelation in ferrioxamine E. Figure 2 shows that in the crystalline state the configuration is cis; the same configuration is found for the hydroxamate chelation in ferrichroma A[18] and in iron(III) benzhydroxamate.[19] Equivalent bond distances in the hydroxamate groups agree very well with the exception of Fe-O(31), which is significantly longer than Fe-O(21) and Fe-O(11) by 8 standard deviations. Correcting the distances for thermal motion (legend Figure 1) does not eliminate this discrepancy. The average uncorrected bond distances (Å) can be compared with those in Fe(III) benzhydroxamate and ferrichrome A (in parentheses): Fe-O$^-$ 1.959 (1.98, 1.98), Fe-O 2.055 (2.06, 2.04), N-O$^-$ 1.381 (1.37, 1.38), C-O 1.275 (1.28, 1.28), C-N 1.307 Å (1.32, 1.32). The bonds around C(i1) (i is 1, 2, and 3) are perfectly planar, while those around N(i1) are approximately in a plane. The difference between the Fe-O(i1) and Fe-O(i2) distances indicates that the majority of the negative charges reside on the oxime oxygen atoms. Some of the negative charge, however, is located on the carbonyl oxygen atoms as indicated by the planarity of the

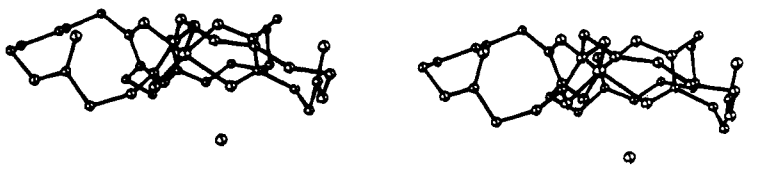

Figure 4. A three-dimensional side view of the molecule using the ORTEP program.[27] Ring I is behind right, II front right, and III left. W(1) is also drawn.

Table II. Bond Angles (Standard deviations for last digit in parentheses.)

Atoms			Indices[a] +0	+10 (mod 30)	+20 (mod 30)
O(11)	Fe	O(12)	79.1 (1)	79.1 (1)	78.6 (1)
O(12)	Fe	O(21)	98.6 (1)	94.6 (1)	97.3 (1)
O(11)	Fe	O(22)	167.5 (1)	167.6 (1)	167.4 (1)
O(11)	Fe	O(21)	91.8 (1)	92.3 (1)	94.4 (1)
O(12)	Fe	O(22)	93.7 (1)	93.1 (1)	91.5 (1)
Fe	O(12)	C(11)	112.5 (3)	112.4 (3)	112.1 (3)
O(12)	C(11)	N(11)	118.2 (4)	118.4 (4)	119.7 (4)
O(12)	C(11)	C(12)	120.5 (4)	121.2 (4)	120.8 (4)
N(11)	C(11)	C(12)	121.2 (4)	120.4 (4)	119.5 (4)
C(11)	N(11)	O(11)	117.4 (4)	116.9 (4)	116.4 (4)
O(11)	N(11)	C(39)	114.4 (4)	113.0 (4)	114.0 (3)
C(11)	N(11)	C(39)	127.6 (4)	129.1 (4)	129.4 (4)
N(11)	O(11)	Fe	111.9 (2)	112.9 (3)	112.9 (2)
C(11)	C(12)	C(13)	113.2 (4)	114.2 (4)	112.8 (4)
C(12)	C(13)	C(14)	113.8 (4)	112.3 (4)	112.2 (4)
C(13)	C(14)	N(12)	116.2 (4)	114.6 (5)	114.8 (4)
C(13)	C(14)	O(13)	120.6 (5)	122.3 (5)	122.0 (4)
O(13)	C(14)	N(12)	123.2 (5)	122.9 (5)	123.2 (5)
C(14)	N(12)	C(15)	125.3 (5)	123.4 (4)	122.3 (4)
N(12)	C(15)	C(16)	112.5 (5)	112.0 (5)	113.6 (5)
C(15)	C(16)	C(17)	119.8 (7)	114.0 (5)	114.3 (5)
C(16)	C(17)	C(18)	115.2 (7)	111.9 (4)	113.0 (4)
C(17)	C(18)	C(19)	118.0 (6)	114.2 (4)	115.2 (4)
C(18)	C(19)	N(21)	109.8 (5)	112.8 (4)	111.9 (4)

[a] For instance the 11th entry in the second column would be O(21) N(21) C(19): 113.0 (4)°.

Table III. Least-Squares Planes

Plane	Atoms in plane	A	B	C	D
1:	Fe, O(12), C(11), N(11), O(11)	16.802	4.466	−1.878	4.327
2:	Fe, O(22), C(21), N(21), O(21)	3.934	−5.934	7.424	0.664
3:	Fe, O(32), C(31), N(31), O(31)	−11.488	7.523	2.314	−1.245

Δ(1) (Å)		Δ(2) (Å)		Δ(3) (Å)	
Fe	0.047	Fe	0.025	Fe	0.028
O(12)	−0.049	O(22)	−0.023	O(32)	−0.031
C(11)	0.020	C(21)	0.006	C(31)	0.017
N(11)	0.040	N(21)	0.026	N(31)	0.019
O(11)	−0.059	O(21)	−0.033	O(31)	−0.033

[a] The planes are expressed in the form $Ax + By + Cz = D$, in which x, y, and z are fractional coordinates and D is the distance from the plane to the origin.

bonds around the N(i1) atoms. The least-squares planes of the five-membered rings show these rings to be all in the envelope conformation (Table III).

The macrocycles can be thought to be formed by the condensation of an 1-amino-5-hydroxylaminopentane group and a succinyl group forming a peptide linkage in each ring. The bond distances in the peptide groups show definite differences of 8 standard deviations, but the average values of the C′—N and C′=O bonds of 1.331 and 1.228 Å agree quite well with the average values for a peptide bond[26] of 1.325 and 1.24 Å. The bond distances and bond angles involving C(16), C(17), and C(18) are not reliable due to high thermal motion or disorder of these atoms.

The similarities and differences of the three rings I, II, and III can be inspected with the torsion angles shown in Figure 3. It can be seen that the conformation of II and III is the same, but different from I in that in the latter the conformation of C(16)-C(17) is syn-clinal instead of antiperiplanar and the one of C(18)-C(19) is − and + syn-clinal for I, and II and III, respectively, with the opposite conformations in the symmetry related molecule. Smaller differences exist for C(13)-C(14), N(12)-C(15), and C(19)-N(21) when compared to the similar bonds in II and III. The result is that the pentane chains in II and III are straight which is not the case in I (Figures 1 and 4).

The most noticeable feature of the structure is the flatness of the molecule (Figure 4). The total thickness is only 3.6 Å. The three peptide groups are trans, and the peptide hydrogen atoms are at the lower side of the molecule. All peptide carbonyl groups are pointed up and the oxime oxygen atoms are at that same side of the molecule. These polar groups located on the top part of the molecule are interlaced on that side by the lipophyllic pentane groups. These dual characteristics of that surface of the molecule are most likely important for the transport of the compound through the cell wall. The iron chelation brings the molecule into a relatively rigid and possibly unique conformation, which in the future has to be compared with the one of deferrioxamine E.

All peptide hydrogen atoms are involved in hydrogen bonding: N(12)-O(31) (x,y,z − 1: 2.97 Å), N(22)-O(13) (x,y − 1,z: 2.92 Å), and N(32)-O(32) ($\bar{x},\bar{y},\bar{z}$: 3.10 Å). W(1) makes an hydrogen bond with O(13) of 2.83 Å and has contacts with O(22) and O(32) at 3.07 and 3.16 Å. W(2) forms two hydrogen bonds with O(23) of two symmetry related molecules. There are no other intermolecular contacts less than 3.2 Å for the nonhydrogen atoms.

Acknowledgment. We thank Dr. Keller-Schierlein for making the compound available to us. Part of the research was supported by a grant, GM-21822, and a development award, GM-42572, both, from the National Institutes of Health. We thank the University of Oklahoma for providing computing facilities.

Supplementary Material Available: listing of the structure factor amplitudes (16 pages). Ordering information is given on any current masthead page.

References and Notes

(1) J. B. Neilands in "Inorganic Biochemistry," Vol. I, G. L. Eichhorn, Ed., Elsevier, New York, N.Y., 1973, p 167.
(2) T. Emery, *Adv. Enzymol.*, **35**, 135 (1971).
(3) J. B. Neilands, *J. Am. Chem. Soc.*, **74**, 4846 (1952).
(4) J. A. Garibaldi and J. B. Neilands, *Nature (London)*, **177**, 526 (1956).
(5) V. Prelog, *Pure Appl. Chem.*, **6**, 327 (1963).
(6) J. B. Neilands, *Bacteriol. Rev.*, **21**, 101 (1957).
(7) T. Emery, *Biochemistry*, **10**, 1483 (1971).
(8) H. Bickel, R. Bosshardt, E. Gäumann, P. Reusser, E. Vischer, W. Voser, A. Wettstein, and H. Zähner, *Helv. Chim. Acta*, **43**, 2118 (1960).
(9) W. Keller-Schierlein and V. Prelog, *Helv. Chim. Acta*, **45**, 590 (1962).
(10) H. Bickel, G. E. Hall, W. Keller-Schierlein, V. Prelog, E. Vischer, and A. Wettstein, *Helv. Chim. Acta*, **43**, 2129 (1960).
(11) W. Keller-Schierlein and V. Prelog, *Helv. Chim. Acta*, **44**, 709 (1961).

(12) W. Keller-Schierlein and V. Prelog, *Helv. Chim. Acta*, **44**, 1981 (1961).
(13) V. Prelog and A. Walser, *Helv. Chim. Acta*, **45**, 631 (1962).
(14) W. Keller-Schierlein and V. Prelog, *Helv. Chim. Acta*, **45**, 1732 (1962).
(15) W. Keller-Schierlein, P. Mertens, V. Prelog, and A. Walser, *Helv. Chim. Acta*, **48**, 710 (1965).
(16) T. F. Emery, *Biochemistry*, **6**, 3858 (1967).
(17) M. Llinas, M. P. Klein, and J. B. Neilands, *J. Mol. Biol.*, **52**, 399 (1970).
(18) A. Zalkin, J. D. Forrester, and D. H. Templeton, *J. Am. Chem. Soc.*, **88**, 1810 (1966).
(19) H. J. Lindner and S. Göttlicher, *Acta Crystallogr., Sect. B*, **25**, 832 (1969).
(20) P. Coppens, L. Leiserowitz, and D. Rabinovich, *Acta Crystallogr.*, **18**, 1035 (1965).
(21) F. R. Ahmed, SFLS program, NCR-10, National Research Council, Ottawa, 1966.
(22) A. L. Patterson, *Acta Crystallogr.*, **16**, 1255 (1963).
(23) "International Tables for X-Ray Crystallography", Vol. III, Kynoch Press, Birmingham, 1962, pp 202, 214.
(24) D. van der Helm and H. B. Nicholas, *Acta Crystallogr., Sect. B*, **26**, 1858 (1970).
(25) See paragraph at the end of paper regarding supplementary material.
(26) R. E. Marsh and J. Donohue, *Adv. Protein Chem.*, **22**, 235 (1967).
(27) C. K. Johnson, ORTEP Report ORNL-3794, Oak Ridge National Laboratory, Oak Ridge, Tenn.

The Reactivity of Cobalt(I) Complexes Containing Unsaturated Macrocyclic Ligands in Aqueous Solution[1]

A. Martin Tait,[2a] Morton Z. Hoffman,*[2a] and E. Hayon*[2b]

Contribution from the Department of Chemistry, Boston University, Boston, Massachusetts 02215, and the Pioneering Research Laboratory, U.S. Army Natick Laboratories, Natick, Massachusetts 01760. *Received January 27, 1975*

Abstract: The fast kinetics technique of pulse radiolysis has been used to generate and characterize, in aqueous solution, Co(I) complexes containing the tetradentate 14-membered macrocyclic ligands 5,7,7,12,14,14-hexamethyl-1,4,8,11-tetraazacyclotetradeca-4,11-diene (4,11-dieneN$_4$), 5,7,7,12,12,14-hexamethyl-1,4,8,11-tetraazacyclotetradeca-4,14-diene (4,14-dieneN$_4$), and 2,3,9,10-tetramethyl-1,4,8,11-tetraazacyclotetradeca-1,3,8,10-tetraene (1,3,8,10-tetraeneN$_4$). The reaction of the hydrated electron, e_{aq}^-, with the Co(II) complexes ($k \sim 5 \times 10^{10}$ M^{-1} sec^{-1}) produces the corresponding Co(I) species. Co^{I}(1,3,8,10-tetraeneN$_4$) is also generated by the action of CO_2^- and $(CH_3)_2\dot{C}OH$ radicals on Co(II). The absorption spectra of these monovalent complexes have been determined and their decay kinetics studied as a function of pH and added scavengers. The Co(I) species behave as bases, reacting with proton donors such as H_3O^+, CH_3CO_2H, $H_2PO_4^-$, NH_4^+, HPO_4^{2-}, and H_2O. They also behave as powerful reducing agents, transferring an electron ($k \sim 10^9$ to 10^6 M^{-1} sec^{-1}) to a variety of organic acceptors and one-electron metal complex oxidants such as Fe(III), Co(III), Cr(III), and Ru(III) amine, bipyridyl, and macrocyclic complexes. The Co(I) species react rapidly with N_2O, CH_3I, and O_2.

The chemistry of cobalt complexes containing macrocyclic or tetradentate ligands with delocalized electronic structures may be taken as an approximate model for the reactions of vitamin B_{12} in biochemical processes.[3,4] Among the oxidation states of cobalt, the Co(I) state has been proposed as a reaction intermediate in the reduction of cobaloxime and aquocobalamin by CO[5,6] and in biological processes as vitamin B_{12S}.[4,7] Co(I) species display strong nucleophilic character, readily displacing halide ions from alkyl halides producing cobalt-alkyl complexes.[8-10] The catalytic role of some Co(I) complexes has recently been demonstrated in the reduction of several alkyl ammonium ions[10] and in the conversion of nitrogen and acetylene to ammonia and ethylene.[11]

It has previously been reported[12,13] that Co(I) complexes containing the macrocyclic ligands 4,11-dieneN$_4$ and aneN$_4$[14] are exceptionally reactive and powerful reducing agents and cannot be handled in protic solvents when generated electrochemically from the corresponding Co(II) complexes. Because of their short lifetimes, these species, or any other Co(I) macrocyclic species, have not been characterized in aqueous solution.

The technique of pulse radiolysis is well suited to the study of such highly reactive low-valent species. The radiolysis of water provides a means of selectively generating one-electron reducing or oxidizing agents. The hydrated electron, e_{aq}^-, is produced directly by the ionizing radiation and is a powerful reducing agent ($E_{ox}^0 = 2.8$ V).[17] Other reductants, such as CO_2^- and $(CH_3)_2\dot{C}OH$ radicals, can be generated by the reaction of OH radicals, produced in the radiation pulse, with HCO_2^- and $(CH_3)_2CHOH$, respectively.[18,19] The reactions of the radicals with solutes, such as coordination complexes, can be monitored using fast kinetics absorption spectrophotometry with a time resolution of ~0.1 μsec enabling the spectra of short-lived transient intermediates to be observed and their kinetics characterized.

In this paper we describe the reactions of Co(II) complexes containing the 4,11-dieneN$_4$, 4,14-dieneN$_4$, and 1,3,8,10-tetraeneN$_4$ macrocyclic ligands with reducing radicals to generate the corresponding Co(I) species in aqueous solution. The spectra and reactivities of these low-valent complexes are examined in detail. It is important to note that the tetradentate equatorial ligand renders macrocyclic complexes of this type stable towards displacement of the ligand from the metal center so that at least the macrocyclic structure maintains its integrity upon change of the oxidation state of the metal.

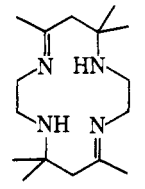

Me$_6$[14]4,11-diene N$_4$

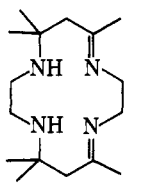

Me$_6$[14]4,14-dieneN$_4$

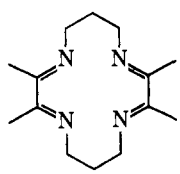

Me$_4$[14]1,3,8,10-tetraene N$_4$

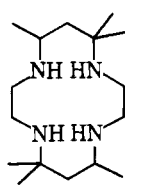

Me$_6$[14]aneN$_4$